

# UCLA

## UCLA Previously Published Works

### Title

Characterization of the Spectrum of Ophthalmic Changes in Patients With Alagille Syndrome.

### Permalink

<https://escholarship.org/uc/item/43p780wz>

### Journal

Investigative Ophthalmology and Visual Science, 62(7)

### Authors

da Palma, Mariana  
Igelman, Austin  
Ku, Cristy  
et al.

### Publication Date

2021-06-01

### DOI

10.1167/iovs.62.7.27

Peer reviewed

# Characterization of the Spectrum of Ophthalmic Changes in Patients With Alagille Syndrome

Mariana Matioli da Palma,<sup>1,2</sup> Austin D. Igelman,<sup>1</sup> Cristy Ku,<sup>1</sup> Amanda Burr,<sup>1</sup> Jia Yue You,<sup>3</sup> Emily M. Place,<sup>4</sup> Nan-Kai Wang,<sup>5</sup> Jin Kyun Oh,<sup>5,6</sup> Kari E. Branham,<sup>7</sup> Xinxin Zhang,<sup>8</sup> Jeeyun Ahn,<sup>9,10</sup> Michael B. Gorin,<sup>9,11</sup> Byron L. Lam,<sup>12</sup> Cecinio C. Ronquillo,<sup>13</sup> Paul S. Bernstein,<sup>13</sup> Aaron Nagiel,<sup>14,15</sup> Rachel Huckfeldt,<sup>4</sup> Michelle T. Cabrera,<sup>16,17</sup> John P. Kelly,<sup>17</sup> Benjamin Bakall,<sup>18</sup> Alessandro Iannaccone,<sup>8</sup> Robert B. Hufnagel,<sup>19</sup> Wadih M. Zein,<sup>19</sup> Robert K. Koenekoop,<sup>3</sup> David G. Birch,<sup>20</sup> Paul Yang,<sup>1</sup> Abigail T. Fahim,<sup>7</sup> and Mark E. Pennesi<sup>1</sup>

<sup>1</sup>Casey Eye Institute, Oregon Health & Science University, Portland, Oregon, United States

<sup>2</sup>Department of Ophthalmology and Visual Sciences, Federal University of São Paulo (UNIFESP), São Paulo, SP, Brazil

<sup>3</sup>Departments of Ophthalmology, Human Genetics, and Pediatric Surgery, Montreal Children's Hospital, McGill University Health Centre, McGill University, Montreal, QC, Canada

<sup>4</sup>Department of Ophthalmology, Massachusetts Eye and Ear, Harvard Medical School, Boston, Massachusetts, United States

<sup>5</sup>Department of Ophthalmology, Edward S. Harkness Eye Institute, Columbia University Irving Medical Center, New York, New York, United States

<sup>6</sup>State University of New York, Downstate Medical Center, Brooklyn, New York, United States

<sup>7</sup>Department of Ophthalmology and Visual Sciences, Kellogg Eye Center, University of Michigan, Ann Arbor, Michigan, United States

<sup>8</sup>Duke Eye Center, Department of Ophthalmology, Duke University School of Medicine, Durham, North Carolina, United States

<sup>9</sup>UCLA Stein Eye Institute, Division of Retinal Disorders and Ophthalmic Genetics, Department of Ophthalmology, David Geffen School of Medicine, UCLA, Los Angeles, California, United States

<sup>10</sup>Department of Ophthalmology, Seoul National University, College of Medicine, Seoul Metropolitan Government Seoul National University Boramae Medical Center, Seoul, Korea

<sup>11</sup>Department of Human Genetics, David Geffen School of Medicine, UCLA, Los Angeles, California, United States

<sup>12</sup>Bascom Palmer Eye Institute, University of Miami, Miami, Florida, United States

<sup>13</sup>John A. Moran Eye Center, University of Utah, Salt Lake City, Utah, United States

<sup>14</sup>The Vision Center, Department of Surgery, Children's Hospital Los Angeles, Los Angeles, California, United States

<sup>15</sup>Roski Eye Institute, Department of Ophthalmology, University of Southern California, Los Angeles, California, United States

<sup>16</sup>Department of Ophthalmology, University of Washington, Seattle, Washington, United States

<sup>17</sup>Department of Ophthalmology, Seattle Children's Hospital, Seattle, Washington, United States

<sup>18</sup>Department of Ophthalmology, University of Arizona College of Medicine, Phoenix, Arizona, United States

<sup>19</sup>Ophthalmic Genetics and Visual Function Branch, National Eye Institute, National Institutes of Health, Bethesda, Maryland, United States

<sup>20</sup>Retina Foundation of the Southwest, Dallas, Texas, United States

Correspondence: Mark E. Pennesi, Casey Eye Institute, Oregon Health & Science University, 515 SW Campus Dr Portland, OR 97239, USA; [pennesim@ohsu.edu](mailto:pennesim@ohsu.edu).

**Received:** February 3, 2021

**Accepted:** June 6, 2021

**Published:** June 29, 2021

Citation: da Palma MM, Igelman AD, Ku C, et al. Characterization of the spectrum of ophthalmic changes in patients with Alagille syndrome. *Invest Ophthalmol Vis Sci.* 2021;62(7):27. <https://doi.org/10.1167/iovs.62.7.27>

**PURPOSE.** The purpose of this study was to characterize the phenotypic spectrum of ophthalmic findings in patients with Alagille syndrome.

**METHODS.** We conducted a retrospective, observational, multicenter, study on 46 eyes of 23 subjects with Alagille syndrome. We reviewed systemic and ophthalmologic data extracted from medical records, color fundus photography, fundus autofluorescence, optical coherence tomography, visual fields, electrophysiological assessments, and molecular genetic findings.

**RESULTS.** Cardiovascular abnormalities were found in 83% of all cases (of those, 74% had cardiac murmur), whereas 61% had a positive history of hepatobiliary issues, and musculoskeletal anomalies were present in 61% of all patients. Dysmorphic facies were present in 16 patients, with a broad forehead being the most frequent feature. Ocular symptoms were found in 91%, with peripheral vision loss being the most frequent complaint. Median (range) Snellen visual acuity of all eyes was 20/25 (20/20 to hand motion [HM]). Anterior segment abnormalities were present in 74% of the patients; of those, posterior embryotoxon was the most frequent finding. Abnormalities of the optic disc were found in 52%, and peripheral retinal abnormalities were the most frequent ocular finding in

this series, found in 96% of all patients. Fifteen *JAG1* mutations were identified in 16 individuals; of those, 6 were novel.

**CONCLUSIONS.** This study reports a cohort of patients with Alagille syndrome in which peripheral chorioretinal changes were more frequent than posterior embryotoxon, the most frequent ocular finding according to a number of previous studies. We propose that these peripheral chorioretinal changes are a new hallmark to help diagnose this syndrome.

**Keywords:** Alagille syndrome, retinal dystrophies, jaundice, cholestasis

Alagille syndrome (ALGS, OMIM 118450) was first described by Daniel Alagille,<sup>1</sup> who began studying patients with biliary disease in 1956.<sup>2</sup> A study published in 1975 described 15 patients with one of the hallmarks of the syndrome, intrahepatic bile duct hypoplasia causing persistent cholestasis.<sup>3</sup> In addition, patients were noted to have other features, such as characteristic triangular facies, cardiac murmur, vertebral arch defects, intellectual disability, and hypogonadism.<sup>2</sup> The ocular features of ALGS were discovered later<sup>4</sup> and form part of the criteria for diagnosing this disorder.<sup>5,6</sup> The classic criteria to diagnose ALGS were established in 1987 and required a paucity of the interlobular bile ducts and at least three of five major features, which included chronic cholestasis, cardiac disease, anomalies of the vertebrae, characteristic facial phenotype, and ocular abnormalities.<sup>7-9</sup> Posterior embryotoxon, characterized by a prominent and anterior Schwalbe's line at the junction of the corneal endothelium and the uveal trabecular meshwork,<sup>9</sup> is a major criterion and has been reported as the most frequent ocular finding.<sup>6,10-12</sup> However, some studies have reported that the presence of optic disc drusen on ocular ultrasound may be more common than posterior embryotoxon in ALGS.<sup>13-15</sup> Other ocular abnormalities that have been reported include a mosaic pattern of iris stromal hypoplasia, corectopia, microcornea, strabismus, high myopia, pigmentary retinopathy,<sup>13,16</sup> and geographic chorioretinopathy.<sup>10</sup> Using wide-field imaging, Esmaili documented one patient with peripheral chorioretinal atrophy that extended circumferentially bilaterally with a sharp demarcation between the normal and abnormal retina in the periphery.<sup>16</sup> However, the frequency of peripheral chorioretinal atrophy has not been previously reported.

The incidence of ALGS is estimated between 1 in 30,000 and 70,000 live births and is inherited in an autosomal dominant pattern.<sup>17</sup> The majority (greater than 90%) of the cases result from pathogenic variants in the Jagged canonical Notch ligand 1 (*JAG1*) gene on chromosome 20p12.<sup>18</sup> About 7% of cases have deletions in chromosome 20 that include this gene.<sup>19</sup> Only a few cases have reported pathogenic variants in NOTCH receptor 2 (*NOTCH2*) gene on chromosome 1p12.<sup>20-22</sup> Gilbert et al. also described a few molecularly uncharacterized individuals.<sup>21</sup>

The transmembrane proteins encoded by these two genes<sup>21</sup> play a role in cell signaling during embryonic development, notably in the Notch signaling pathway.<sup>23</sup> This is a highly conserved pathway<sup>24,25</sup> that regulates cell proliferation, fate, and differentiation<sup>25</sup> during different stages of embryogenesis.<sup>9,26</sup> The protein encoded by *JAG1* is a Delta ligand for the Notch receptor(s).<sup>5,10,27,28</sup> The protein encoded by *NOTCH2* is a receptor that mediates molecular signaling between cells.<sup>29</sup> Mutations in these genes

contribute to various systemic issues possibly due to a loss of cellular interactions. However, the exact molecular mechanism of how these genes act in embryogenesis and throughout life is not well established.<sup>8,30</sup>

ALGS is genetically and phenotypically heterogeneous.<sup>26</sup> The clinical diagnosis of ALGS is difficult given the variability in the clinical presentation, even among family members who can have incomplete features of this disease and can even be unaffected.<sup>19,31,32</sup> The rate of germline mosaicism might be relatively high, and the penetrance low.<sup>31</sup> The availability of genetic testing aids in diagnosing this multisystem syndrome in patients that do not fit the classic clinical spectrum. Early diagnosis can contribute to early interventions to prevent complications in multiple organs and better follow-up.<sup>27,32</sup>

This study presents 23 patients with ALGS across different ophthalmic clinics with examination findings and multimodal imaging findings to characterize the anterior and posterior segment characteristics of this ultra-rare inherited disorder.

## METHODS

This retrospective study across different institutions was conducted at Casey Eye Institute in Oregon Health & Science University (OHSU). The research was approved by the institutional review boards at all participating centers and was performed following the Declaration of Helsinki and protection of the patient's identity. De-identified clinical history, clinical findings, ocular imaging, and genetic test results were collected and analyzed.

### Case Identification

Medical records of confirmed cases of ALGS were reviewed by inherited eye disease specialists. For all cases, demographic variables, such as age, history of consanguinity, positive or negative family history, systemic clinical findings, and genetic testing results, were extracted from medical records. Data from ophthalmologic findings included ocular symptoms, best-corrected visual acuity (BCVA), intraocular pressure (IOP), and ocular examination.

### Image Analysis

Images from 46 eyes of 23 patients were used for this study. Because our cohort consisted of patients from different centers, available images varied widely between subjects. Color fundus photography, fundus autofluorescence (FAF), and optical coherence tomography (OCT) were assessed for detailed phenotyping. Kinetic visual field and full-field

TABLE 1. Molecular and Systemic Features of Patients With Alagille Syndrome

ID	JAG1 DNA Variant and Protein Change	Hepatobiliary Issues	Dysmorphic Facies	Cardiovascular Issues	Musculoskeletal Issues
1	c.1713dupC	Hyperbilirubinemia	Flat nasal bridge	Murmur, pulmonary artery stenosis, ASD	None
121185	c.Cys572Leufs*2	Liver transplant	Broad forehead, deep-set eyes, flat nasal bridge, pointed chin	Murmur, pulmonary artery stenosis, VSD	None
2	c.1268_1269insA	Liver transplant	Broad forehead, deep-set eyes, pointed chin	Murmur, pulmonary artery stenosis, ASD	Axial skeleton anomalies
3	p.Asn423Lysfs*6 No mutation found	Liver transplant	Broad forehead, prominent ears, straight nose, pointed chin	Murmur with aortic rand tricuspid regurgitation	Spina bifida
4	Not available	Cholestasis	Broad forehead, pointed chin	None	Neck/back/joint pain
5	Not tested	Liver transplant	Straight nose	Murmur	None
6	c.2587dupT	Liver transplant	Broad forehead, deep-set eyes, pointed chin	Murmur, pulmonary artery stenosis	Chronic osteomyelitis
7*	p.Cys863Leufs*16 Not tested	Liver transplant	Broad forehead, deep-set eyes, prominent ears, straight nose, bulbous tip, pointed chin	Murmur, pulmonary artery stenosis	None
22496	c.2694C>A	None	Not documented	Pulmonary artery stenosis	None
8	p.Cys883*	Cholestasis	Broad forehead, deep-set eyes, prominent ears	Murmur, pulmonary artery stenosis	Short stature, joint dislocation
10981	Not tested	Cholestasis	Broad forehead, deep-set eyes, prominent ears	Murmur, pulmonary artery stenosis, VSD, tetralogy of Fallot	Scoliosis
9	Not tested	Liver transplant	Broad forehead, deep-set eyes, prominent ears, straight nose	Murmur	None
10	Not tested	Liver transplant	Broad forehead, hypertelorism, pointed chin	Murmur, pulmonary artery stenosis, VSD, tetralogy of Fallot	None
11*	c.439+1G>A	None	Broad forehead, deep-set eyes, prominent ears, straight nose	Murmur	None
29177	c.719dupC	Jaundice, cholestasis, hyperbilirubinemia	Broad forehead, deep-set eyes, prominent ears, straight nose	Murmur, VSD	None
12	p.Lys241* c.3234dupT	None	Broad forehead, deep-set eyes, straight nose, bulbous tip, pointed chin	Murmur, pulmonary artery stenosis, VSD	Axial skeleton anomalies, shoulder sprain, ankle injury
22710	p.Val1079Cysfs*30				

TABLE 1. Continued

ID	JAG1 DNA Variant and Protein Change	Hepatobiliary Issues	Dysmorphic Facies	Cardiovascular Issues	Musculoskeletal Issues
14 <sup>‡</sup>	c.2473 C>T (p.Gln825*)	None	Not documented	Murmur	Scoliosis
15	Not available	Jaundice, cholestasis, hyperbilirubinemia	Broad forehead, deep-set eyes, straight nose, bulbous tip, pointed chin	Murmur, pulmonary artery stenosis	Axial skeleton anomalies, Pectus excavatum, scoliosis, Scoliosis, butterfly vertebrae
16	c.1899_1900delTG	Cholestasis, hepatosplenomegaly	None	Murmur, pulmonary artery stenosis, VSD	Scoliosis, butterfly vertebrae
129354	p.Cys633*	Liver transplant	Broad forehead, deep-set eyes, pointed chin	None	None
17	c.1191delG	None	Not documented	None	None
18	p.Lys397Asnfs*15	None	Not documented	Hypertension	None
OG12357_003916	c.1395+3A>G	None	Not documented	None	None
19	c.2066del	None	Not documented	Hypertension	None
15070	p.Phe689Serfs*54	Jaundice, hyperbilirubinemia	Broad forehead, deep-set eyes, prominent ears, straight nose, bulbous tip	None	Short stature
20	c.2698C>T	None	Not documented	None	None
21	p.Arg900* c.1563_1564del p.Cys522Serfs*8	None	None	Murmur, bicuspid aortic valve	Mild scoliosis, degenerative disc disease
22	c.2230C>T (p.Arg744*)	None	Broad forehead, deep-set eyes, straight nose	Mitral disease, Subclavian vein thrombosis	Scoliosis, degenerative disc disease
23 <sup>†</sup>	c.2473 C>T (p.Gln825*)	None	Not documented	Right bundle block	Scoliosis, arthritis

Abbreviations: ASD, atrial septal defect; VSD, ventral septal defect.

Symbols: \*siblings; †father and ‡daughter.

TABLE 2. Ophthalmic Features of Patients With Alagille Syndrome

ID	Age y	Visual Acuity OD OS	Ocular Symptoms	Anterior Segment Features	Optic Disc Findings	Macular Features (Fundus Exam and OCT Findings)	Peripheral Retinal Changes
1	3	Not tested	Nyctalopia	Posterior embryotoxon Iris stromal hypoplasia	Elevated disc	Pericentral ring of atrophy and EZ loss surrounding fovea	Pigment mottling
2	8	20/40 20/40	Nyctalopia, photophobia, peripheral vision issues	Normal	Elevated disc	Normal	Blonde
3	9	20/20 20/20	Failed vision screen	Normal	Anomalous nerve	Normal	Chorioretinal atrophy
4	9	20/20 20/20	Negative	Posterior embryotoxon	Not elevated, horizontally oval shaped	Thin choroid	Tessellated
5	11	20/40 20/25	Decreased vision, nyctalopia, peripheral vision issues	Posterior embryotoxon	Normal	Mild atrophy at peripheral edge	Severe atrophy of outer retina
6	12	20/50 20/25	Decreased vision, nyctalopia, peripheral vision issues	Posterior embryotoxon	Elevated disc	Thin macula with RPE dropout	RPE atrophy and bone-spicule pigment like deposits
7	12	20/20 20/20	Decreased vision, photophobia	Posterior embryotoxon Iris stromal hypoplasia	Elevated disc	Hypopigmented macula area	Peripheral hypopigmen- tation
8	13	20/40 20/100	Decreased vision, nyctalopia, peripheral vision issues	Normal	Swelling of the disc	RPE changes and EZ loss; VMT OS	Pigmentary changes, bone spiculing
9	14	20/30 20/25	Peripheral vision issues	Posterior embryotoxon	Normal	Granular changes, xanthophyllic pigmentation	Bone spicules
10	14	20/40 20/40	Decreased vision, photophobia, peripheral vision issues	Posterior embryotoxon Cortical cataract OU	Elevated disc	Mild atrophy	Pigment and RPE changes with retinal thinning

TABLE 2. Continued

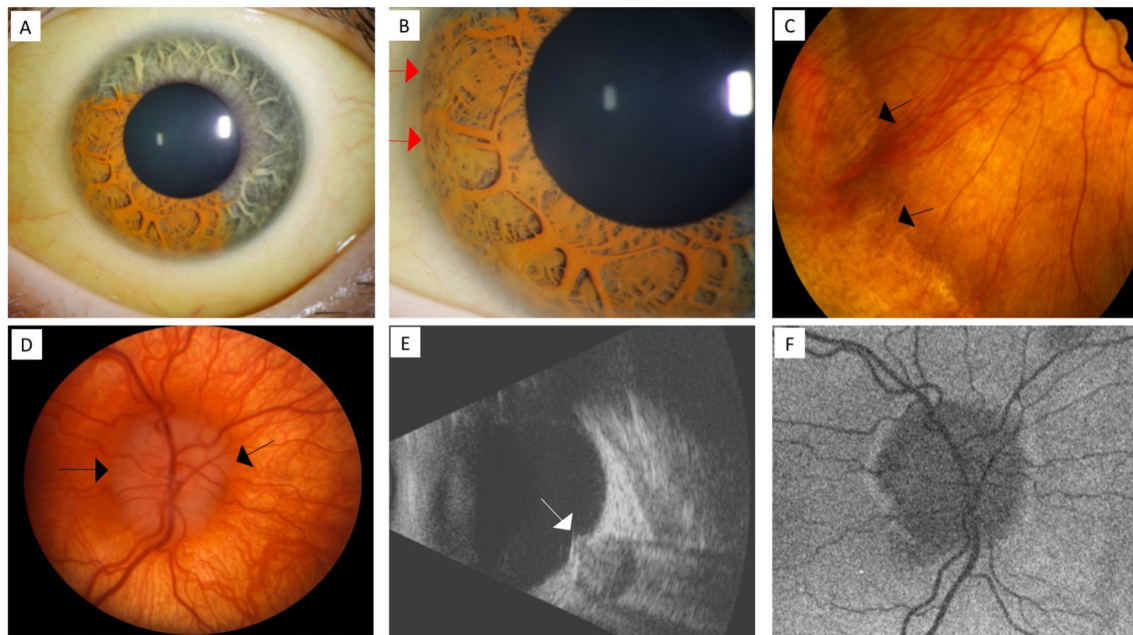
ID	Age y	Visual Acuity OD OS	Ocular Symptoms	Anterior Segment Features	Optic Disc Findings	Macular Features (Fundus Exam and OCT Findings)	Peripheral Retinal Changes
11	15	20/25 20/20	Decreased vision, peripheral vision issues	Posterior embryotoxon	Elevated disc	Normal	Far periphery atrophy with nummular patches and pigmentary changes
12	16	20/20 20/20	Negative	Posterior embryotoxon Iris stromal hypoplasia	Normal	Normal	None
13	19	20/25 20/25	Decreased vision, photophobia	Posterior embryotoxon PSC cataract OU	Optic nerve drusen	Very mild mottling	Well-demarcated chorioretinal atrophy
14	19	20/20 20/50	Decreases vision, nyctalopia, photophobia, peripheral vision, and color vision issues	Posterior embryotoxon	Normal	Pigment mottling at fovea, surrounded by RPE atrophy	Circumscribed chorioretinal atrophy 360° starting in mid-periphery
15	22	20/25 20/20	Nyctalopia, photophobia, peripheral vision issues	Posterior embryotoxon Iris stromal hypoplasia	Normal	Mild EZ abnormality close to peripheral border of the macula	Wedge shape chorioretinal atrophy
16	22	20/20 20/20	Photophobia	Normal	Normal	Normal	Nasal pigment mottling
17	29	20/70 HM	Decreases vision, nyctalopia, photophobia, peripheral vision, and color vision issues	PSC cataract OU	Normal	Diffuse atrophy	Diffuse atrophy OU, asteroid OS

TABLE 2. Continued

ID	Age y	Visual Acuity OD OS	Ocular Symptoms	Anterior Segment Features	Optic Disc Findings	Macular Features (Fundus Exam and OCT Findings)	Peripheral Retinal Changes
18	34	20/50 20/50	Decreased vision, nyctalopia, peripheral vision issues	Posterior embryotoxon PSC cataract OU	Normal	Pigmented changes and EZ loss surrounding fovea	Atrophic with bone spicules
19	36	20/25 20/25	Decreased vision, peripheral vision issues	Normal	Normal	Staphyloma and pigmented changes; Isolated cyst OD	RPE atrophy, bone spicules
20	37	20/30 20/40	Peripheral vision issues	Posterior embryotoxon Microcornea	Optic nerve drusen	PPA atrophic changes extending to nasal macula	Pigment redistribution and
21	41	20/25 20/25	Nyctalopia	Normal	Optic nerve drusen	Pigmented changes	Bone spicules
22	49	20/25 20/40	Decreased vision, nyctalopia, peripheral vision, and color vision issues	Posterior embryotoxon PCIOL	Normal	Patchy parafoveal RPE atrophy	Well circumscribed chorioretinal atrophy 360° starting in mid-periphery
23	52	20/400 20/800	Decreased vision, peripheral vision, and color vision issues	Posterior embryotoxon Iris stromal hypoplasia PCIOL	Normal	Central pigment changes OU	Extensive peripheral atrophy OU

Abbreviations: OD, right eye; OS, left eye; OU, both eyes; HM, hand motion; EZ, ellipsoid zone; RPE, retinal pigment epithelium; VMT, vitreomacular traction syndrome; PPA, peripapillary atrophy; PCIOL, posterior chamber intraocular lens.





**FIGURE 1.** Anterior and posterior chamber findings of Alagille syndrome in two siblings. Patient 7 (A–C) with scleral icterus, iris stromal hypoplasia A, and posterior embryotoxon (red arrows) B. Fundus photograph showing a well-demarcated wave border between normal and abnormal retina in the periphery C. Patient 11 (D–F) with an elevated optic disc (black arrows) in the fundus photograph at age 7 D, ultrasonography showing the elevation in optic nerve head (white arrow) E, and autofluorescence 8 years later showing no hyperautofluorescence (i.e. no signal of optic disc drusen) F.

electroretinogram (ffERG) performed according to International Society for Clinical Electrophysiology of Vision (ISCEV) standards<sup>35</sup> were also analyzed.

### Molecular Analysis

Nucleotide and protein changes collected from medical records were described as recommended by the Human Genome Variation Society (HGVS). The variants found were compared with variations listed in the Human Gene Mutation Database (HGMD) and ClinVar. The VarSome Software was used to investigate the pathogenicity of the variants. The variants are reported as “pathogenic,” “likely pathogenic,” “uncertain significance,” “likely benign,” and “benign.”<sup>34</sup> The frequency was evaluated using gnomAD.

## RESULTS

### Clinical Findings

Clinical features are summarized in Table 1. Twenty-three patients with a confirmed diagnosis from 21 families were evaluated. Sixteen patients with conclusive molecular testing and seven patients that met clinical criteria for ALGS. The study population was comprised of 11 male subjects and 12 female subjects. Their ages at the last review with ophthalmic pictures ranged from 3 to 52 years (mean = 22; median = 16).

**Systemic Findings.** Systemic history of hepatobiliary issues, cardiovascular abnormalities, skeletal abnormalities, and dysmorphic facies were collected based on the subject’s chart information. These findings are summarized in Table 1.

Hepatobiliary issues were reported in 14 patients (61% of 23), including jaundice, hyperbilirubinemia, cholestasis,

hepatosplenomegaly, and liver failure, requiring transplantation. Cardiovascular abnormalities were found in 83% (19/23) of the patients. Among those, heart murmur was the most frequent cardiovascular finding presented in 74% (14/19), pulmonary artery stenosis was presented in 53% (10/19), ventricular septal defect in 26% (5/19), and two patients presented with atrial septal defect. Musculoskeletal anomalies were present in 61% of the patients and included butterfly vertebrae, scoliosis, spina bifida, short stature, fractures, and chronic osteomyelitis. Sixteen patients were described with dysmorphic facies; of those, broad forehead was the most frequent finding in 88% (14/16) of the cases; deep-set eyes were present in 69% (11/16); straight nose in 56% (9/16); pointed chin in 56% (9/16); prominent ears in 38% (6/16); and bulbous tip in 25% (4/16). Dysmorphic facies were not present in two patients and there was no comment in the clinic notes about facial characteristics in records from five patients.

**Ophthalmologic Findings.** These findings are summarized in Table 2. The majority of patients (91%) presented with ocular symptoms, except two patients (patients 4 and 12). Nyctalopia was reported in 48% (11/23) of the subjects and was more frequent than photophobia, which was reported in 35% (8/23) of the patients. Peripheral vision problems were present in 73% of 22 subjects (one patient was unable to assess).

The BCVA in each eye ranged from 20/20 to hand motion (HM). The BCVA of the youngest patient was not tested. From 44 eyes tested, the plurality of the eyes (30%) was 20/20. The median Snellen visual acuity of all tested eyes was 20/25, and the mean was 20/40. Most eyes (39 of 44 [89%]) had a BCVA of 20/50 or better. The BCVA of patient 17 was 20/70 and HM. This patient had diffuse macula atrophy and the worst visual acuity of our series. The IOP ranged

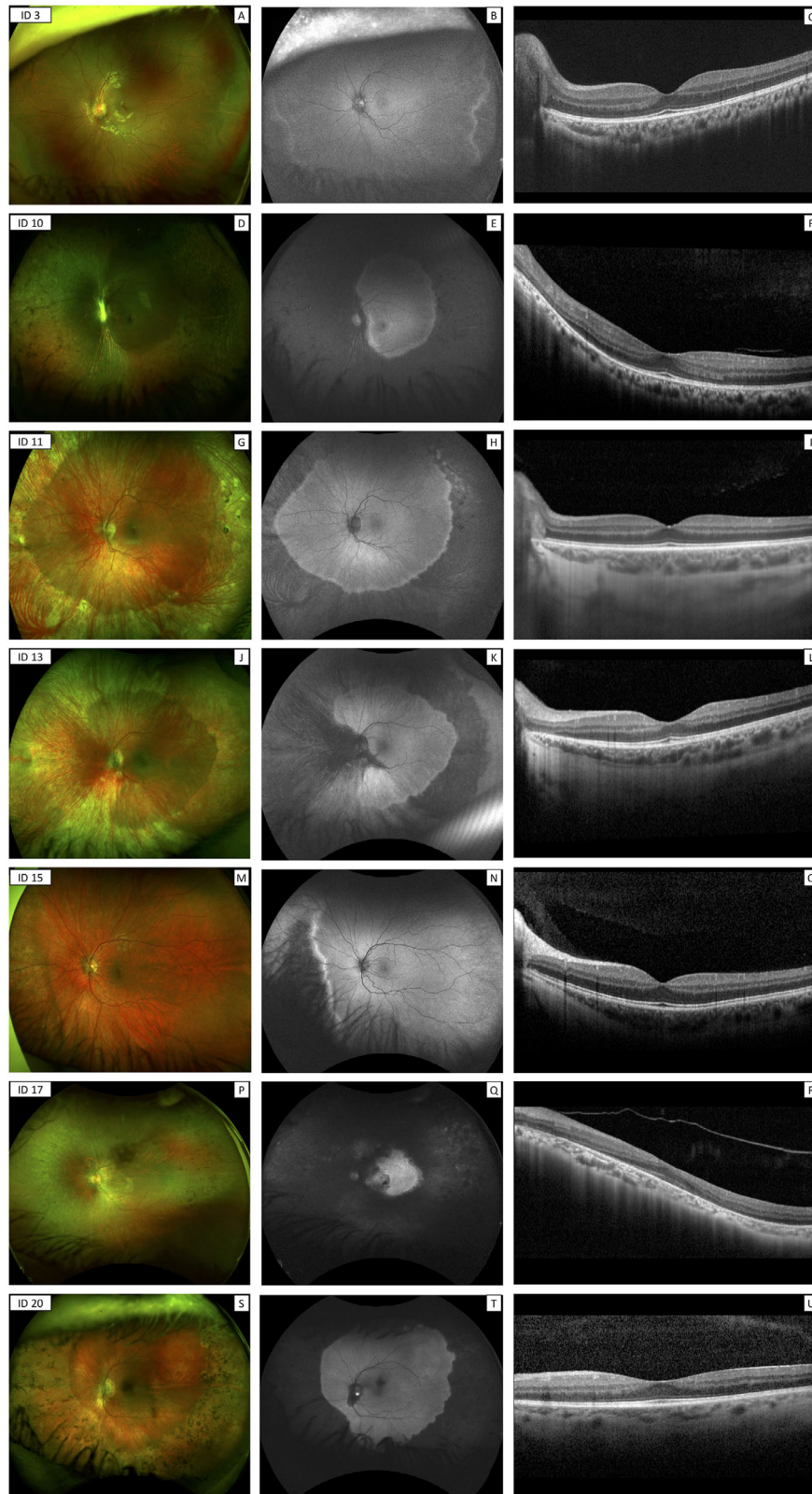


**FIGURE 2.** Multimodal imaging in the left eye of patients with Alagille syndrome. Patient 3 (A–C) at 9-years-old presenting with tortuosity of the retinal vessels and hypopigmented changes in the retinal periphery on fundus photography **A**. Autofluorescence (FAF) showing a wave border in the periphery separating peripheral hyperautofluorescence from posterior normal autofluorescence **B**. Optical coherence tomography (OCT) revealed a normal retina structure at the fovea **C**. Patient 10 (D–F) at 14-years-old presented with attenuated retinal vessels and pigmentary changes with bone spicules on fundus photography **D**. FAF demonstrated circumferential hyperautofluorescence in the mid-periphery and periphery **E**. OCT identified ellipsoid zone (EZ) granularities temporal to the fovea and loss of EZ nasal to the fovea **F**. Patient 11 (G–I) at 15-years-old presented with chorioretinal atrophy in the periphery with few pigmentary changes **G**. FAF showed



circumferential autofluorescence loss **H**. OCT demonstrated normal retinal structure (**I**). Patient 13 (**J–L**) at 19-years-old presented with attenuated retinal vessels nasally, circumferential chorioretinal atrophy in the periphery, and atrophy from inferior nasal to optic disc on fundus photography **J**. FAF demonstrated autofluorescence loss circumferentially and nasal to the optic disc **K**. OCT showed mild EZ abnormality near the optic disc **L**. Patient 16 (**M–O**) at 22-years-old presented with peripheral retinal changes, mainly nasally on fundus photographs **M**. FAF demonstrated a wave border between normal and abnormal retina **N**. OCT showed normal retina structure **O**. Patient 18 (**P–R**) at 34-years-old presented with attenuated vessels and diffuse atrophic appearance of the retina with bone spicules **P**. FAF showed the most severe loss of autofluorescence **Q**. OCT was characterized by loss of foveal contour and outer retinal atrophy surrounding the fovea **R**. Patient 21 (**S–U**) at 41-years-old presented with well-demarcated peripheral chorioretinal changes with bone spicules in the periphery on fundus photography **S**. FAF demonstrated well-demarcated hypoautofluorescence in the periphery **T**. OCT showed normal retina structure **U**.

from 8 to 22 mm Hg (mean = 16; median = 16). Only one eye had a measurement of IOP higher than 21 mm Hg.

Anterior segment findings were present in 74% (17/23) of patients. Posterior embryotoxon (Fig. 1B) was the most common anterior chamber abnormality and presented in 70% (16/23) of patients. Microcornea was present only in one subject, and iris stromal hypoplasia was present in five patients (22%; see Fig. 1A). A total of four patients had bilateral cataracts (17%). The most frequent type of cataract was posterior subcapsular. Two patients (patients 22 and 23) were pseudophakic in both eyes due to cataract surgeries, which occurred in their fifth decade of life.

Posterior segment abnormalities were reported in 96% (22/23) of the patients. Abnormalities of the optic disc were found in 12 patients (52%). These abnormalities were described as optic nerve drusen in three patients, elevated disc in six, anomalous nerve in one, swelling of the optic disc in one, and horizontally oval shaped in another one patient. Macular appearance varied from normal (22%) to diffuse atrophy, and 78% of all patients presented with macular changes including atrophy, pigmented, mottling, and granular changes. One patient (patient 19) presented with an isolated optic cyst in the OCT. Patient 8 presented with vitreomacular traction syndrome in the left eye and low visual acuity. All patients underwent OCT in our cohort. Peripheral retinal abnormalities were the most frequent ocular finding in this series, reported in 22 subjects (96%). Only patient 12 had a description of normal periphery. Peripheral retinopathy was best seen with wide-field autofluorescence that showed peripheral hyperautofluorescent areas with well-demarcated borders that corresponded with areas of peripheral chorioretinal atrophy symmetrically in both eyes (Fig. 2). Not all patients had wide-field images available. Only 13 patients underwent wide-field color and autofluorescent wide-field pictures. Three patients underwent fundus autofluorescence of the posterior pole. Seven patients underwent no wide-field color pictures (Table in the Supplementary Material). Retinal function was assessed using kinetic visual fields (Fig. 3) and full-field electroretinogram. Among nine individuals that underwent visual field, it correlated well with intact areas of autofluorescence. Among 17 patients that underwent electroretinography, 14 patients demonstrated abnormal recordings with a pattern of rod-cone dysfunction, with rod responses being more decreased than cone responses, whereas 2 patients had isolated rod dysfunction (patients 9 and 21). Patient 2, the youngest patient that underwent fERG, presented with normal rod and cone dependent responses.

### Molecular Findings

*JAG1* mutations were identified in 16 individuals. We identified six novel variants not reported in the disease-

related variation databases, such as ClinVar and HGMD. These included two nonsense variants c.2694C>A (p.Cys883\*), and c.719dupC (p.Lys241\*); 4 frameshift variants c.1713dupC (p.Cys572Leufs\*2), c.3234dupT (p.Val1079Cysfs\*30), c.1268\_1269insA (p.Asn423Lysfs\*6), and c.2066del (p.Phe689Serfs\*54). The remaining 10 patients presented with previously reported variants: c.2230C>T (p.Arg744\*),<sup>31</sup> c.2473 (p.Gln825\*),<sup>31</sup> c.1899\_1900delTG (p.Cys633\*),<sup>35</sup> c.2698C>T (p.Arg900\*),<sup>35</sup> c.1191delG (p.Lys397Asnfs\*15),<sup>36</sup> c.1563\_1564del (p.Cys522Serfs\*8),<sup>37</sup> c.2587dupT (p.Cys863Leufs\*16),<sup>38</sup> c.439+1G>A,<sup>39</sup> and c.1395+3A>G.<sup>35,39</sup> None of the patients presented with *NOTCH2* mutations. Four patients were not tested. No mutation was found in patient 3. In two patients, molecular findings were not available.

### DISCUSSION

*JAG1* gene contains 26 exons that code for a 1218 amino acid protein. The protein consists of several evolutionarily conserved domains without mutational hotspots.<sup>36</sup> From the 16 patients with conclusive genetic testing, 6 mutations found were classified as novel variants in *JAG1* gene. All of them were absent from the gnomAD database. Most of the mutations found in our study introduce premature stop codons. This finding is consistent with previous reports.<sup>21,35</sup> Pathogenic variants in *JAG1* are commonly protein-truncating, including frameshift, nonsense, small deletions, and less commonly missense or whole gene deletions.<sup>21</sup> Both whole gene deletions and intragenic pathogenic variants can cause similar phenotypes due to a haploinsufficiency of *JAG1*. Until now, no genotype-phenotype correlations have been noted with *JAG1* mutations neither *NOTCH2*.<sup>21</sup>

The classic ocular finding of ALGS is posterior embryotoxon, a malformation related to neural crest defects.<sup>30</sup> Posterior embryotoxon, an asymptomatic feature, can be found in 8 to 15% of normal individuals.<sup>15</sup> Optic disc drusen are a frequent finding in this disease.<sup>6,13</sup> In this large series, we identified an additional common feature of ALGS. Almost all patients in our series presented with well-demarcated peripheral chorioretinal changes that were better seen by FAF. Although this peripheral chorioretinal atrophy has been reported before,<sup>16,40,41</sup> the frequency was unknown and there have only been limited reports of progression.<sup>10</sup> There have been reports of peripheral changes before, Puklin showed this well demarcated peripheral changes in 1981.<sup>40</sup> Thirty-three years after Esmaili showed for the first time using wide field FAF the autofluorescence loss in the periphery of a patient with ALGS.<sup>16</sup> Makino and colleagues also showed the same pattern of peripheral autofluorescence loss and macular involvement extending to peripapillary region in a sleep-mask appearance.<sup>41–43</sup> Interestingly, we found this

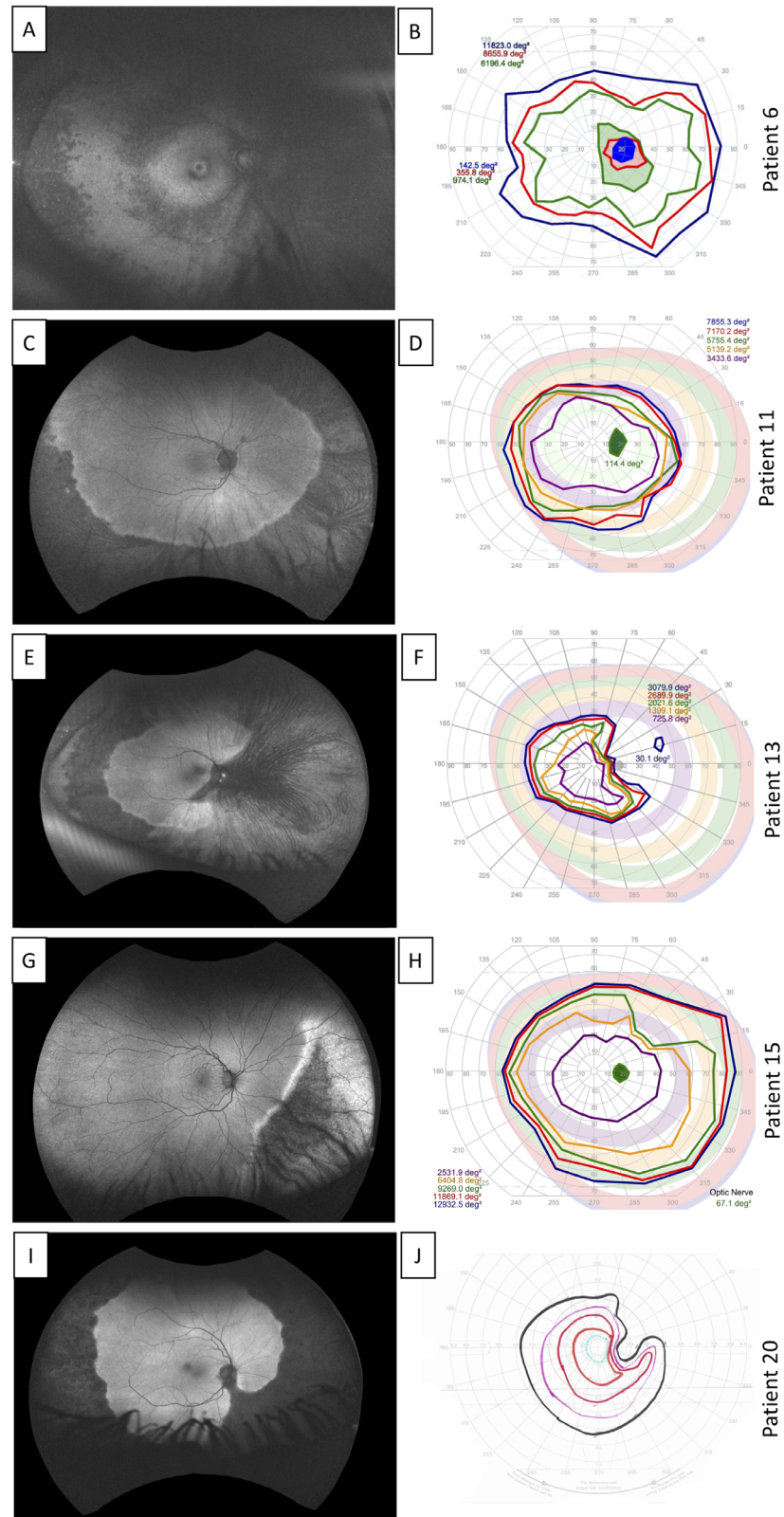


**FIGURE 3.** The visual field responses correlated with intact areas of autofluorescence in Alagille syndrome. Patient 6 (**A, B**). Autofluorescence (FAF) in the right eye (OD) showing hypoautofluorescent spots in the periphery and around the vessels, and macular involvement with a hypoautofluorescent ring surrounding the fovea **A**. The kinetic visual field (KVF) in the right eye showed a central scotoma that corresponds to the macular involvement **B**. Patient 11 (**C, D**). FAF OD demonstrated circumferential peripheral hypoautofluorescence **C**. KVF OD showed mildly constricted isopters to all targets that correspond to peripheral dysfunction **D**. Patient 13 (**E, F**). FAF OD showed circumferential peripheral hypoautofluorescence and loss of autofluorescence nasal to the optic disc **E**. KVF OD showed moderately constricted isopters to all targets, mainly temporal, corresponding to nasal chorioretinal changes **F**. Patient 16 (**G, H**). FAF OD showed inferior nasal hypoautofluorescence **G**. KVF OD demonstrated superior temporal constricted isopter to I4e that probably corresponds to the loss of autofluorescence in the inferior nasal area **H**. Patient 21 (**I, J**). FAF OD showed circumferential peripheral hypoautofluorescence and loss of autofluorescence nasal to the optic disc **I**. KVF shows constriction to all targets, mostly superior temporal, in a pattern corresponding to the autofluorescence loss.

sleep-mask appearance in just few cases. The majority of our patients presented with loss of autofluorescence mainly in the periphery. Our cross-sectional study suggests that this atrophy is progressive in a centripetal direction, but longitudinal studies in the same patients are necessary to confirm this. Hingorani study examined 22 children from ages 5 months to 15 years and found a lower rate of changes in the periphery than we found studying patients from ages 3 to 52 years.<sup>13</sup> It is possible that atrophy was not present in younger ages. On the other hand, an autopsy of a 7-month-old boy with ALGS due to *JAG1* mutation found thin, atrophic, and hypopigmented RPE with speckled hyperpigmentation scattered throughout the retina, especially in the periphery.<sup>5</sup> Additionally, an autopsy of a 6-year-old boy found extensive retinal pigmentary changes, with a demarcation line 4 mm posterior to the equator sparing the central retina.<sup>11</sup> Another reason that we likely found more peripheral changes is that wide-field cameras are now available to more easily inspect the far periphery.

There is a paucity of information about the ophthalmologic spectrum of symptoms and visual function in ALGS with chorioretinopathy. Esmaili did not describe poor night vision or poor peripheral vision.<sup>16</sup> Orssaud reported three patients from the same family with ALGS presenting with narrowing of the peripheral fields<sup>44</sup> and Elshatory reported a case with constricted fields to less than 10 degrees in the right eye and less than 5 degrees in the left eye.<sup>45</sup> We found more nyctalopia than photophobia in our series, and decreased peripheral vision was the most frequent symptom found in 73% of the patients. This symptom was supported by loss of kinetic visual fields. There is also a paucity of information on the ERG abnormalities in existing literature. The retinal disease involves both rods and cones. We found 82% of rod-cone dysfunction and only 12% with isolated rod dysfunction (Table in the Supplementary Material).

Little is known about the underlying pathological mechanism that might cause chorioretinal atrophy in this disease. In an autopsy of a 6-year-old patient, Johnson et al. found massive accumulation of lipofuscin in the RPE and Bruch membrane in the peripheral and equatorial zones of the retina.<sup>11</sup> Although the mechanism that causes this accumulation is uncertain, it is known that accumulation of lipofuscin leads to toxic effects in RPE and ultimately photoreceptors.<sup>46</sup>

Alternatively, the pathogenesis of the chorioretinal atrophy in the periphery with loss of visual field may be associated with progressive vascular abnormality leading to anatomic and functional loss. Researchers showed that interfering in the Notch signaling pathway in mouse models causes retinal dysplasia and that this pathway plays a critical role in retinal vascular development.<sup>47</sup> Vascular retinal abnormalities have been described in patients with ALGS.<sup>13,40</sup> Additionally, cardiac and noncardiac vascular anomalies are also associated with ALGS and therefore vasculopathy has been proposed to be the primary abnormality in ALGS.<sup>48</sup> Elshatory et al. has already presented a case with choroidal bilateral neovascularization reinforcing the involvement of notch pathway in vascular homeostasis.<sup>45</sup>

Cardiac and hepatic abnormalities are the findings that most impact mortality and morbidity.<sup>32</sup> El-Koofy reported the presence of cardiac murmur only in 38% of the patients.<sup>6</sup> This incidence was lower than that reported by Emerick, who found cardiac murmurs in 97% of the patients with a wide variety of cardiovascular anomalies.<sup>12</sup> We found that 61% (14/23) of patients had a cardiac murmur based on chart review. Interestingly, we also found intrafamilial variability

in our study. The affected brother (patient 11) of patient 7, who died after a liver transplant, did not present with hepatobiliary issues. He presented with a cardiac murmur, posterior embryotoxon, and peripheral circumferential chorioretinal atrophy, which triggered his diagnosis.

This study suggests that the presence of peripheral chorioretinal atrophy may be useful for diagnosing ALGS in older children and adults. The retrospective nature of this study, the small sample size, inevitable given the rarity of this syndrome, and the variable multimodal imaging from different institutions prevented characterization of these abnormalities over time. Nonetheless, this study is the largest case series of ALGS focusing on multimodal retinal findings with detailed characterization of this previously described chorioretinal pathology. Additional studies are necessary to determine the progression of the peripheral dystrophy in a longitudinal follow-up.

In summary, ALGS has variable expression, and not all patients have the classic phenotype. We found that a characteristic peripheral chorioretinal degeneration that correlates with loss of function in the visual field is common in patients with ALGS. Posterior changes in the periphery were more common than posterior embryotoxon, an asymptomatic and classic feature. An ophthalmologic evaluation with multimodal retinal imaging should be pursued for all patients suspected to have ALGS.

### Acknowledgments

The authors thank the patients and families for taking part in this research. R.B.H. and W.M.Z. also wish to thank the support of Delphine Blain, ScM, MBA.

**Grants and Funding:** M.M.P. for this study was financed in part by the Coordenação de Aperfeiçoamento de Pessoa de Nível Superior – Brazil (Capes) – Finance Code 001. N.K.W. was supported by the research grant R01EY031354 from National Eye Institute, USA. P.S.B. and C.C.R. received a departmental grant from Research to Prevent Blindness. C.C.R. received the Heed Fellowship. A.N. This work was supported in part by an unrestricted grant to the Department of Ophthalmology at the USC Keck School of Medicine from Research to Prevent Blindness, New York, NY, and the Las Madras Endowment in Experimental Therapeutics for Ophthalmology. M.T.C. received unrestricted grants from Research to Prevent Blindness and the NIH Core Grant EY001730 to the University of Washington Department of Ophthalmology. J.P.K. was supported by an unrestricted grant from grant from the Peter LeHaye, Barbara Anderson, the William O. Rogers Endowment Funds. R.B.H. and W.M.Z. are supported by the intramural research program of the National Eye Institute, National Institutes of Health (NIH). R.K.K. was supported by the Fighting Blindness Canada and NIH (R01030499-01). D.G.B. was supported by the NIH EY009076. P.Y. was supported by grant P30 EY010572 from the National Institutes of Health (Bethesda, MD), and by unrestricted departmental funding from Research to Prevent Blindness (New York, NY) NIH K08EY026650, and the Foundation Fighting Blindness Career Development Award CD-NMT-0714-0648. A.T.F. received grant K12EY022299.

**Disclosure:** M.M. da Palma, None; A.D. Igelman, None; C. Ku, None; A. Burr, None; J.Y. You, None; E.M. Place, None; N.-K. Wang, None; J.K. Oh, None; K.E. Branham, ProQR (C), and serves on the advisory board for Foundation Fighting Blindness; X. Zhang, None; J. Ahn, None; M.B. Gorin, None; B.L. Lam, None; C.C. Ronquillo, None; P.S. Bernstein, None; A. Nagiel, Allergan Retina (C), Biogen (C), and Regenxbio (C); R. Huckfeldt, None; M.T. Cabrera, None; J.P. Kelly, None; B. Bakall,



None; **A. Iannaccone**, None; **R.B. Hufnagel**, None; **W.M. Zein**, None; **R.K. Koenekoop**, None; **D.G. Birch**, Biogen (C), Nacuity (C), ProQR (C), Editas (C), AGTC (C), Iveric (C), Roche-4D (C); **P. Yang**, Adverum (C), AGTC (C), and Nanoscope Therapeutics (C); **A.T. Fahim**, None; **M.E. Pennesi**, serves of the scientific advisor boards for Atsena, DTx Therapeutics, Endogena, Eyevensys, Horama, Nayan, Nacuity Pharmaceuticals, Ocugen, Sparing Vision, and Vedere; **M.E. Pennesi**, serves on advisory board for Foundation Fighting Blindness (this relationship has been reviewed and managed by OHSU), Adverum (C), AGTC (C), Allergan/Editas (C), Astellas Pharmaceuticals (C), Biogen, BlueRock (C), IVERIC (C), Novartis (C), Ora (C), RegenexBio (C), Roche (C), and Viewpoint Therapeutics (C); **M.E. Pennesi**, receives clinical trial support from AGTC, Biogen, Editas, Foundation Fighting Blindness, ProQR, and Sanofi. **M.E. Pennesi**, serves on advisory boards for Foundation Fighting Blindness

## References

- Alagille D, Borde J, Habib EC, Thomassin N. Surgical attempts in atresia of the intrahepatic bile ducts with permeable extrahepatic bile duct. Study of 14 cases in children. *Arch Fr Pediatr*. 1969;26(1):51-71.
- Alagille D, Odièvre M, Gautier M, Dommergues JP. Hepatic ductular hypoplasia associated with characteristic facies, vertebral malformations, retarded physical, mental, and sexual development, and cardiac murmur. *J Pediatr*. 1975;86(1):63-71.
- Humpreys R, Zheng W, Prince LS, et al. Cranial neural crest ablation of Jagged1 recapitulates the craniofacial phenotype of Alagille syndrome patients. *Hum Mol Genet*. 2012; 21(6):1374-1383.
- Riely CA, Cotlier E, Jensen PS, Klatskin G. Arteriohepatic dysplasia: a benign syndrome of intrahepatic cholestasis with multiple organ involvement. *Ann Intern Med*. 1979; 91(4):520-527.
- Ho DK, Levin AV, Anninger WV, Piccoli DA, Eagle RC. Anterior chamber pathology in Alagille syndrome. *Ocul Oncol Pathol*. 2016;2(4):270-275.
- El-Koofy NM, El-Mahdy R, Fahmy ME, El-Hennawy A, Farag MY, El-Karakasy HM. Alagille syndrome: clinical and ocular pathognomonic features. *Eur J Ophthalmol*. 2011;21(2):199-206.
- Alagille D, Estrada A, Hadchouel M, Gautier M, Odièvre M, Dommergues JP. Syndromic paucity of interlobular bile ducts (Alagille syndrome or arteriohepatic dysplasia): review of 80 cases. *J Pediatrics*. 1987;110(2):195-200.
- Penton AL, Leonard LD, Spinner NB. Notch signaling in human development and disease. *Semin Cell Dev Biol*. 2012; 23(4):450-457.
- Jones EA, Clement-Jones M, Wilson DI. JAGGED1 expression in human embryos: correlation with the Alagille syndrome phenotype. *J Med Genet*. 2000;37(9):658-662.
- Bidaguren A, Blanco A, Gibelalde A, Irigoyen C. Progressive geographic chorioretinopathy associated with Alagille syndrome. *Arch Soc Esp Ophthalmol*. 2007;82(8):513-515.
- Johnson BL. Ocular pathologic features of arteriohepatic dysplasia (Alagille's syndrome). *Am J Ophthalmol*. 1990;110(5):504-512.
- Emerick KM, Rand EB, Goldmuntz E, Krantz ID, Spinner NB, Piccoli DA. Features of Alagille syndrome in 92 patients: frequency and relation to prognosis. *Hepatology*. 1999;29(3):822-829.
- Hingorani M, Nischal KK, Davies A, et al. Ocular abnormalities in Alagille syndrome. *Ophthalmology*. 1999; 106(2):330-337.
- El-Karakasy H, Hamed D, Fouad H, Mogahed E, Helmy H, Hasanain F. Ocular findings in patients with cholestatic disorders of infancy: a single-centre experience. *Arab J Gastroenterol*. 2017;18(2):108-113.
- Nischal KK, Hingorani M, Bentley CR, et al. Ocular ultrasound in Alagille syndrome. *Ophthalmology* 1997;104(1):79-85.
- Esmaili D. Chorioretinal atrophy in Alagille syndrome. *Retin Cases Brief Rep*. 2015;9(4):330-332.
- Kamath BM, Baker A, Houwen R, Todorova L, Kerkar N. Systematic review: the epidemiology, natural history, and burden of Alagille syndrome. *J Pediatr Gastroenterol Nutr*. 2018;67(2):148-156.
- Oda T, Elkahoulou AG, Pike BL, et al. Mutations in the human Jagged1 gene are responsible for Alagille syndrome. *Nat Genet*. 1997;16(3): 235-242.
- Li L, Krantz ID, Deng Y, et al. Alagille syndrome is caused by mutations in human Jagged1, which encodes a ligand for Notch1. *Nat Genet*. 1997;16(3):243-251.
- McDaniell R, Warthen DM, Sanchez-Lara PA, et al. NOTCH2 mutations cause Alagille syndrome, a heterogeneous disorder of the notch signaling pathway. *Am J Hum Genet*. 2006;79(1):169-173.
- Gilbert MA, Bauer RC, Rajagopalan R, et al. Alagille syndrome mutation update: comprehensive overview of JAG1 and NOTCH2 mutation frequencies and insight into missense variant classification. *Human Mutat*. 2019;40(12):2197-2220.
- Ahn KJ, Yoon JK, Kim GB, et al. Alagille syndrome and JAG1 mutation: 41 cases of experience at a single center. *Korean J Pediatr*. 2015;58(10):392-397.
- Vajro P, Ferrante L, Paoletta G. Alagille syndrome: an overview. *Clin Res Hepatol Gastroenterol*. 2012;36(3):275-277.
- Manderfield LJ, High FA, Engelka KA, et al. Notch activation of Jagged1 contributes to the assembly of the arterial wall. *Circulation* 2012;125(2):314-323.
- Bray SJ. Notch signaling: a simple pathway becomes complex. *Nat Rev Mol Cell Biol*. 2006;7(9):678-689.
- Kamath BM, Thiel BD, Gai X, et al. SNP array mapping of 20p deletions: genotypes, phenotypes and copy number variation. *Hum Mutat*. 2009; 30(3):371-378.
- Micaglio E, Andronache AA, Carrera P, et al. Novel JAG1 deletion variant in patient with atypical Alagille syndrome. *Int J Mol Sci*. 2019;20(24):pii:E6247.
- Bales CB, Kamath BM, Munoz PS, et al. Pathologic lower extremity fractures in children with Alagille syndrome. *J Pediatr Gastroenterol Nutr*. 2010; 51(1):66-70.
- Gilbert MA, Spinner NB. Alagille syndrome: genetics and functional models. *Curr Pathobiol Rep*. 2017; 5(3): 233-241.
- Andersson ER, Chivukula IV, Hankeeva S, et al. Mouse model of Alagille syndrome and mechanisms of Jagged1 missense mutations. *Gastroenterology*. 2018;154(4):1080-1095.
- Krantz ID, Colliton RP, Genin A, et al. Spectrum and frequency of Jagged 1 (JAG1) mutations in Alagille syndrome patients and their families. *Am J Hum Genet*. 1998; 62(6):1361-1369.
- Kamath BM, Bason L, Piccoli DA, Krantz ID, Spinner NB. Consequences of JAG1 mutations. *J Med Genet*. 2003; 40(12):891-895.
- McCulloch DL, Marmor MF, Brigell MG, et al. ISCEV Standard for full-field clinical electroretinography (2015 update). *Doc Ophthalmol*. 2015;130(1):1-12.
- Richards S, Aziz N, Bale S, et al. ACMG Laboratory Quality Assurance Committee. Standards and guidelines for the interpretation of sequence variants: a joint consensus recommendation of the American College of Medical Genetics and Genomics and the Association for Molecular Pathology. *Genet Med*. 2015;17(5):405-424.

35. Crosnier C, Driancourt C, Raynaud N, et al. Mutations in JAGGED1 gene are predominantly sporadic in Alagille syndrome. *Gastroenterology*. 1999;116(5):1141–1148.
36. Colliton RP, Bason L, Lu FM, Piccoli DA, Krantz ID, Spinner NB. Mutation analysis of Jagged1 (JAG1) in Alagille syndrome patients. *Hum Mutat*. 2001;17(2):151–152.
37. Warthen DM, Moore EC, Kamath BM, et al. Jagged1 (JAG1) mutations in Alagille syndrome: increasing the mutation detection rate. *Hum Mutat*. 2006;27(5):436–443.
38. Lin HC, Le Hoang P, Hutchinson A, et al. Alagille syndrome in a Vietnamese cohort: mutation analysis and assessment of facial features. *Am J Med Genet A*. 2012;158A(5):1005–1013.
39. Jurkiewicz D, Gliwicz D, Ciara E, et al. Spectrum of JAG1 gene mutations in Polish patients with Alagille syndrome. *J Appl Genet*. 2014;55(3):329–336.
40. Puklin JE, Riely CA, Simon RM, Cotlier E. Anterior segment and retinal pigmentary abnormalities in arteriohepatic dysplasia. *Ophthalmology*. 1981;88(4):337–347.
41. Makino S, Tampo COH. Peripheral circumferential chorioretinal atrophy in a patient with Alagille syndrome. *Imaging J Clin Med Sciences*. 2016;3(1):009–009.
42. Makino S, Ohkubo Y, Tampo H. Optical coherence tomography and fundus autofluorescence imaging study of chorioretinal atrophy involving the macula in Alagille syndrome. *Clin Ophthalmol*. 2012;6:1445–1448.
43. Sato A, Makino S, Tampo H. Sleep mask-like chorioretinal atrophy in a patient with Alagille syndrome. *J Pediatr Ophthalmol Strabismus*. 2016;53(6):384.
44. Orssaud C, Robert MP, Roche O. Relevance of identifying JAG1 mutations in patients with isolated posterior embryotoxon. *J Glaucoma*. 2016;25(12):923–925.
45. Elshatory YM, Carver A, Shah VA, Aleman TS. Diagnostic and therapeutic challenges. *Retina*. 2016;36(4):840–845.
46. Pichi F, Abboud EB, Ghazi NG, Khan AO. Fundus autofluorescence imaging in hereditary retinal diseases. *Acta Ophthalmol*. 2018;96(5):e549–e561.
47. Zheng M, Zhang Z, Zhao X, Ding Y, Han H. The Notch signaling pathway in retinal dysplasia and retina vascular homeostasis. *J Genet Genomics*. 2010;37(9):573–582.
48. Turnpenny PD, Ellard S. Alagille syndrome: pathogenesis, diagnosis and management. *Eur J Hum Genet*. 2012;20(3):251–257.